

Observation of a state $X(2600)$ in the $\pi^+\pi^-\eta'$ system in the process $J/\psi \rightarrow \gamma\pi^+\pi^-\eta'$

M. Ablikim¹, M. N. Achasov^{10,b}, P. Adlarson⁶⁸, S. Ahmed¹⁴, M. Albrecht⁴, R. Aliberti²⁸, A. Amoroso^{67A,67C}, M. R. An³², Q. An^{64,50}, X. H. Bai⁵⁸, Y. Bai⁴⁹, O. Bakina²⁹, R. Baldini Ferroli^{23A}, I. Balossino^{24A}, Y. Ban^{39,h}, V. Batozskaya^{1,37}, D. Becker²⁸, K. Begzsuren²⁶, N. Berger²⁸, M. Bertani^{23A}, D. Bettoni^{24A}, F. Bianchi^{67A,67C}, J. Bloms⁶¹, A. Bortone^{67A,67C}, I. Boyko²⁹, R. A. Briere⁵, H. Cai⁶⁹, X. Cai^{1,50}, A. Calcaterra^{23A}, G. F. Cao^{1,55}, N. Cao^{1,55}, S. A. Cetin^{54A}, J. F. Chang^{1,50}, W. L. Chang^{1,55}, G. Chelkov^{29,a}, C. Chen³⁶, G. Chen¹, H. S. Chen^{1,55}, M. L. Chen^{1,50}, S. J. Chen³⁵, T. Chen¹, X. R. Chen²⁵, X. T. Chen¹, Y. B. Chen^{1,50}, Z. J. Chen^{20,i}, W. S. Cheng^{67C}, G. Cibinetto^{24A}, F. Cossio^{67C}, J. J. Cui⁴², X. F. Cui³⁶, H. L. Dai^{1,50}, J. P. Dai⁷¹, X. C. Dai^{1,55}, A. Dbeyssi¹⁴, R. E. de Boer⁴, D. Dedovich²⁹, Z. Y. Deng¹, A. Denig²⁸, I. Denysenko²⁹, M. Destefanis^{67A,67C}, F. De Mori^{67A,67C}, Y. Ding³³, C. Dong³⁶, J. Dong^{1,50}, L. Y. Dong^{1,55}, M. Y. Dong^{1,50,55}, X. Dong⁶⁹, S. X. Du⁷³, P. Egorov^{29,a}, Y. L. Fan⁶⁹, J. Fang^{1,50}, S. S. Fang^{1,55}, Y. Fang¹, R. Farinelli^{24A}, L. Fava^{67B,67C}, F. Feldbauer⁴, G. Felici^{23A}, C. Q. Feng^{64,50}, J. H. Feng⁵¹, M. Fritsch⁴, C. D. Fu¹, Y. N. Gao^{39,h}, Yang Gao^{64,50}, I. Garzia^{24A,24B}, P. T. Ge⁶⁹, C. Geng⁵¹, E. M. Gersabeck⁵⁹, A. Gilman⁶², K. Goetzen¹¹, L. Gong³³, W. X. Gong^{1,50}, W. Gradl²⁸, M. Greco^{67A,67C}, M. H. Gu^{1,50}, C. Y. Guan^{1,55}, A. Q. Guo²⁵, A. Q. Guo²², L. B. Guo³⁴, R. P. Guo⁴¹, Y. P. Guo^{9,g}, A. Guskov^{29,a}, T. T. Han⁴², W. Y. Han³², X. Q. Hao¹⁵, F. A. Harris⁵⁷, K. K. He⁴⁷, K. L. He^{1,55}, F. H. Heinsius⁴, C. H. Heinz²⁸, Y. K. Heng^{1,50,55}, C. Herold⁵², M. Himmelreich^{11,e}, T. Holtmann⁴, G. Y. Hou^{1,55}, Y. R. Hou⁵⁵, Z. L. Hou¹, H. M. Hu^{1,55}, J. F. Hu^{48,j}, T. Hu^{1,50,55}, Y. Hu¹, G. S. Huang^{64,50}, L. Q. Huang⁶⁵, X. T. Huang⁴², Y. P. Huang¹, Z. Huang^{39,h}, T. Hussain⁶⁶, N. Hüsken^{22,28}, W. Ikegami Andersson⁶⁸, W. Imoehl²², M. Irshad^{64,50}, S. Jaeger⁴, S. Janchiv²⁶, Q. Ji¹, Q. P. Ji¹⁵, X. B. Ji^{1,55}, X. L. Ji^{1,50}, Y. Y. Ji⁴², H. B. Jiang⁴², S. S. Jiang³², X. S. Jiang^{1,50,55}, J. B. Jiao⁴², Z. Jiao¹⁸, S. Jin³⁵, Y. Jin⁵⁸, M. Q. Jing^{1,55}, T. Johansson⁶⁸, N. Kalantar-Nayestanaki⁵⁶, X. S. Kang³³, R. Kappert⁵⁶, M. Kavatsyuk⁵⁶, B. C. Ke⁷³, I. K. Keshk⁴, A. Khoukaz⁶¹, P. Kiese²⁸, R. Kiuchi¹, R. Kliemt¹¹, L. Koch³⁰, O. B. Kolcu^{54A}, B. Kopf⁴, M. Kuemmel⁴, M. Kuessner⁴, A. Kupsc^{37,68}, M. G. Kurth^{1,55}, W. Kühn³⁰, J. J. Lane⁵⁹, J. S. Lange³⁰, P. Larin¹⁴, A. Lavanaia²¹, L. Lavezzi^{67A,67C}, Z. H. Lei^{64,50}, H. Leithoff²⁸, M. Lellmann²⁸, T. Lenz²⁸, C. Li⁴⁰, C. Li³⁶, C. H. Li³², Cheng Li^{64,50}, D. M. Li⁷³, F. Li^{1,50}, G. Li¹, H. Li^{64,50}, H. Li⁴⁴, H. B. Li^{1,55}, H. J. Li¹⁵, H. N. Li^{48,j}, J. L. Li⁴², J. Q. Li⁴, J. S. Li⁵¹, Ke Li¹, L. J. Li¹, L. K. Li¹, Lei Li³, M. H. Li³⁶, P. R. Li^{31,k,l}, S. X. Li⁹, S. Y. Li⁵³, T. Li⁴², W. D. Li^{1,55}, W. G. Li¹, X. H. Li^{64,50}, X. L. Li⁴², Xiaoyu Li^{1,55}, Z. Y. Li⁵¹, H. Liang^{1,55}, H. Liang^{64,50}, H. Liang²⁷, Y. F. Liang⁴⁶, Y. T. Liang²⁵, G. R. Liao¹², L. Z. Liao^{1,55}, J. Libby²¹, A. Limphirat⁵², C. X. Lin⁵¹, D. X. Lin²⁵, T. Lin¹, B. J. Liu¹, C. X. Liu¹, D. Liu^{14,64}, F. H. Liu⁴⁵, Fang Liu¹, Feng Liu⁶, G. M. Liu^{48,j}, H. M. Liu^{1,55}, Huanhuan Liu¹, Huihui Liu¹⁶, J. B. Liu^{64,50}, J. L. Liu⁶⁵, J. Y. Liu^{1,55}, K. Liu¹, K. Y. Liu³³, Ke Liu¹⁷, L. Liu^{64,50}, M. H. Liu^{9,g}, P. L. Liu¹, Q. Liu⁵⁵, S. B. Liu¹, T. Liu^{1,55}, T. Liu^{9,g}, W. M. Liu^{64,50}, X. Liu^{31,k,l}, Y. Liu^{31,k,l}, Y. B. Liu³⁶, Z. A. Liu^{1,50,55}, Z. Q. Liu⁴², X. C. Lou^{1,50,55}, F. X. Lu⁵¹, H. J. Lu¹⁸, J. D. Lu^{1,55}, J. G. Lu^{1,50}, X. L. Lu¹, Y. Lu¹, Y. P. Lu^{1,50}, Z. H. Lu¹, C. L. Luo³⁴, M. X. Luo⁷², T. Luo^{9,g}, X. L. Luo^{1,50}, X. R. Lyu⁵⁵, Y. F. Lyu³⁶, F. C. Ma³³, H. L. Ma¹, L. L. Ma⁴², M. M. Ma^{1,55}, Q. M. Ma¹, R. Q. Ma^{1,55}, R. T. Ma⁵⁵, X. X. Ma^{1,55}, X. Y. Ma^{1,50}, Y. Ma^{39,h}, F. E. Maas¹⁴, M. Maggiora^{67A,67C}, S. Maldaner⁴, S. Malde⁶², Q. A. Malik⁶⁶, A. Mangoni^{23B}, Y. J. Mao^{39,h}, Z. P. Mao¹, S. Marcello^{67A,67C}, Z. X. Meng⁵⁸, J. G. Messchendorp^{56,d}, G. Mezzadri^{24A}, H. Miao¹, T. J. Min³⁵, R. E. Mitchell²², X. H. Mo^{1,50,55}, N. Yu. Muchnoi^{10,b}, H. Muramatsu⁶⁰, S. Nakhoul^{11,e}, Y. Nefedov²⁹, F. Nerling^{11,e}, I. B. Nikolaev^{10,b}, Z. Ning^{1,50}, S. Nisar^{8,m}, S. L. Olsen⁵⁵, Q. Ouyang^{1,50,55}, S. Pacetti^{23B,23C}, X. Pan^{9,g}, Y. Pan⁵⁹, A. Pathak¹, A. Pathak²⁷, P. Patteri^{23A}, M. Pelizaeus⁴, H. P. Peng^{64,50}, K. Peters^{11,e}, J. Pettersson⁶⁸, J. L. Ping³⁴, R. G. Ping^{1,55}, S. Plura²⁸, S. Pogodin²⁹, R. Poling⁶⁰, V. Prasad^{64,50}, H. Qi^{64,50}, H. R. Qi⁵³, M. Qi³⁵, T. Y. Qi^{9,g}, S. Qian^{1,50}, W. B. Qian⁵⁵, Z. Qian⁵¹, C. F. Qiao⁵⁵, J. J. Qin⁶⁵, L. Q. Qin¹², X. P. Qin^{9,g}, X. S. Qin⁴², Z. H. Qin^{1,50}, J. F. Qiu¹, S. Q. Qu³⁶, K. H. Rashid⁶⁶, K. Ravindran²¹, C. F. Redmer²⁸, K. J. Ren³², A. Rivetti^{67C}, V. Rodin⁵⁶, M. Rolo^{67C}, G. Rong^{1,55}, Ch. Rosner¹⁴, M. Rump⁶¹, H. S. Sang⁶⁴, A. Sarantsev^{29,c}, Y. Schelhaas²⁸, C. Schnier⁴, K. Schoenning⁶⁸, M. Scodeggio^{24A,24B}, K. Y. Shan^{9,g}, W. Shan¹⁹, X. Y. Shan^{64,50}, J. F. Shangguan⁴⁷, L. G. Shao^{1,55}, M. Shao^{64,50}, C. P. Shen^{9,g}, H. F. Shen^{1,55}, X. Y. Shen^{1,55}, B.-A. Shi⁵⁵, H. C. Shi^{64,50}, R. S. Shi^{1,55}, X. Shi^{1,50}, X. D. Shi^{64,50}, J. J. Song¹⁵, W. M. Song^{27,1}, Y. X. Song^{39,h}, S. Sosio^{67A,67C}, S. Spataro^{67A,67C}, F. Stieler²⁸, K. X. Su⁶⁹, P. P. Su⁴⁷, Y.-J. Su⁵⁵, G. X. Sun¹, H. K. Sun¹, J. F. Sun¹⁵, L. Sun⁶⁹, S. S. Sun^{1,55}, T. Sun^{1,55}, W. Y. Sun²⁷, X. Sun^{20,i}, Y. J. Sun^{64,50}, Y. Z. Sun¹, Z. T. Sun⁴², Y. H. Tan⁶⁹, Y. X. Tan^{64,50}, C. J. Tang⁴⁶, G. Y. Tang¹, J. Tang⁵¹, L. Y. Tao⁶⁵, Q. T. Tao^{20,i}, J. X. Teng^{64,50}, V. Thoren⁶⁸, W. H. Tian⁴⁴, Y. T. Tian²⁵, I. Uman^{54B}, B. Wang¹, D. Y. Wang^{39,h}, F. Wang⁶⁵, H. J. Wang^{31,k,l}, H. P. Wang^{1,55}, K. Wang^{1,50}, L. L. Wang¹, M. Wang⁴², M. Z. Wang^{39,h}, Meng Wang^{1,55}, S. Wang^{9,g}, T. J. Wang³⁶, W. Wang⁵¹, W. H. Wang⁶⁹, W. P. Wang^{64,50}, X. Wang^{39,h}, X. F. Wang^{31,k,l}, X. L. Wang^{9,g}, Y. D. Wang³⁸, Y. F. Wang^{1,50,55}, Y. Q. Wang¹, Y. Y. Wang^{31,k,l}, Ying Wang⁵¹, Z. Wang^{1,50}, Z. Y. Wang¹, Ziyi Wang⁵⁵, Zongyuan Wang^{1,55}, D. H. Wei¹², F. Weidner⁶¹, S. P. Wen¹, D. J. White⁵⁹, U. Wiedner⁴, G. Wilkinson⁶², M. Wolke⁶⁸, L. Wollenberg⁴, J. F. Wu^{1,55}, L. H. Wu¹, L. J. Wu^{1,55}, X. Wu^{9,g}, X. H. Wu²⁷, Z. Wu^{1,50}, L. Xia^{64,50}, T. Xiang^{39,h}, H. Xiao^{9,g}, S. Y. Xiao¹, Y. L. Xiao^{9,g}, Z. J. Xiao³⁴, X. H. Xie^{39,h}, Y. G. Xie^{1,50}, Y. H. Xie⁶, T. Y. Xing^{1,55}, C. F. Xu¹, C. J. Xu⁵¹, G. F. Xu¹³, Q. J. Xu¹³, S. Y. Xu⁶³, W. Xu^{1,55}, X. P. Xu⁴⁷, Y. C. Xu⁵⁵, F. Yan^{9,g}, L. Yan^{9,g}, W. B. Yan^{64,50}, W. C. Yan⁷³, H. J. Yang^{43,f}, H. X. Yang¹, L. Yang⁴⁴, S. L. Yang⁵⁵, Y. X. Yang¹², Y. X. Yang^{1,55}, Yifan Yang^{1,55}, Zhi Yang²⁵, M. Ye^{1,50}, M. H. Ye⁷, J. H. Yin¹, Z. Y. You⁵¹, B. X. Yu^{1,50,55}, C. X. Yu³⁶, G. Yu^{1,55}, J. S. Yu^{20,i}, T. Yu⁶⁵, C. Z. Yuan^{1,55}, L. Yuan², S. C. Yuan¹, X. Q. Yuan¹, Y. Yuan¹, Z. Y. Yuan⁵¹, C. X. Yue³², A. A. Zafar⁶⁶, X. Zeng Zeng⁶, Y. Zeng^{20,i}, A. Q. Zhang¹, B. L. Zhang¹, B. X. Zhang¹, G. Y. Zhang¹⁵, H. Zhang⁶⁴, H. H. Zhang⁵¹, H. H. Zhang²⁷, H. Y. Zhang^{1,50}, J. L. Zhang⁷⁰, J. Q. Zhang³⁴, J. W. Zhang^{1,50,55}, J. Y. Zhang¹, J. Z. Zhang^{1,55}, Jianyu Zhang^{1,55}, Jiawei Zhang^{1,55}, L. M. Zhang⁵³, L. Q. Zhang⁵¹, Lei Zhang³⁵, P. Zhang¹, Shulei Zhang^{20,i}, X. D. Zhang³⁸, X. M. Zhang¹, X. Y. Zhang⁴², X. Y. Zhang⁴⁷, Y. Zhang⁶², Y. T. Zhang⁷³, Y. H. Zhang^{1,50}, Yan Zhang^{64,50}, Yao Zhang¹, Z. H. Zhang¹, Z. Y. Zhang³⁶, Z. Y. Zhang⁶⁹, G. Zhao¹, J. Zhao³², J. Y. Zhao^{1,55}, J. Z. Zhao^{1,50}, Lei Zhao^{64,50}, Ling Zhao¹, M. G. Zhao³⁶, Q. Zhao¹, S. J. Zhao⁷³, Y. B. Zhao^{1,50}, Y. X. Zhao²⁵, Z. G. Zhao^{64,50}, A. Zhemchugov^{29,a},

B. Zheng⁶⁵, J. P. Zheng^{1,50}, Y. H. Zheng⁵⁵, B. Zhong³⁴, C. Zhong⁶⁵, L. P. Zhou^{1,55}, Q. Zhou^{1,55}, X. Zhou⁶⁹, X. K. Zhou⁵⁵, X. R. Zhou^{64,50}, X. Y. Zhou³², Y. Z. Zhou^{9,g}, A. N. Zhu^{1,55}, J. Zhu³⁶, K. Zhu¹, K. J. Zhu^{1,50,55}, S. H. Zhu⁶³, T. J. Zhu⁷⁰, W. J. Zhu^{9,g}, W. J. Zhu³⁶, Y. C. Zhu^{64,50}, Z. A. Zhu^{1,55}, B. S. Zou¹, J. H. Zou¹

(BESIII Collaboration)

- ¹ *Institute of High Energy Physics, Beijing 100049, People's Republic of China*
² *Beihang University, Beijing 100191, People's Republic of China*
³ *Beijing Institute of Petrochemical Technology, Beijing 102617, People's Republic of China*
⁴ *Bochum Ruhr-University, D-44780 Bochum, Germany*
⁵ *Carnegie Mellon University, Pittsburgh, Pennsylvania 15213, USA*
⁶ *Central China Normal University, Wuhan 430079, People's Republic of China*
⁷ *China Center of Advanced Science and Technology, Beijing 100190, People's Republic of China*
⁸ *COMSATS University Islamabad, Lahore Campus, Defence Road, Off Raiwind Road, 54000 Lahore, Pakistan*
⁹ *Fudan University, Shanghai 200443, People's Republic of China*
¹⁰ *G.I. Budker Institute of Nuclear Physics SB RAS (BINP), Novosibirsk 630090, Russia*
¹¹ *GSI Helmholtzcentre for Heavy Ion Research GmbH, D-64291 Darmstadt, Germany*
¹² *Guangxi Normal University, Guilin 541004, People's Republic of China*
¹³ *Hangzhou Normal University, Hangzhou 310036, People's Republic of China*
¹⁴ *Helmholtz Institute Mainz, Staudinger Weg 18, D-55099 Mainz, Germany*
¹⁵ *Henan Normal University, Xinxiang 453007, People's Republic of China*
¹⁶ *Henan University of Science and Technology, Luoyang 471003, People's Republic of China*
¹⁷ *Henan University of Technology, Zhengzhou 450001, People's Republic of China*
¹⁸ *Huangshan College, Huangshan 245000, People's Republic of China*
¹⁹ *Hunan Normal University, Changsha 410081, People's Republic of China*
²⁰ *Hunan University, Changsha 410082, People's Republic of China*
²¹ *Indian Institute of Technology Madras, Chennai 600036, India*
²² *Indiana University, Bloomington, Indiana 47405, USA*
²³ *INFN Laboratori Nazionali di Frascati, (A)INFN Laboratori Nazionali di Frascati, I-00044, Frascati, Italy; (B)INFN Sezione di Perugia, I-06100, Perugia, Italy; (C)University of Perugia, I-06100, Perugia, Italy*
²⁴ *INFN Sezione di Ferrara, (A)INFN Sezione di Ferrara, I-44122, Ferrara, Italy; (B)University of Ferrara, I-44122, Ferrara, Italy*
²⁵ *Institute of Modern Physics, Lanzhou 730000, People's Republic of China*
²⁶ *Institute of Physics and Technology, Peace Ave. 54B, Ulaanbaatar 13330, Mongolia*
²⁷ *Jilin University, Changchun 130012, People's Republic of China*
²⁸ *Johannes Gutenberg University of Mainz, Johann-Joachim-Becher-Weg 45, D-55099 Mainz, Germany*
²⁹ *Joint Institute for Nuclear Research, 141980 Dubna, Moscow region, Russia*
³⁰ *Justus-Liebig-Universitaet Giessen, II. Physikalisches Institut, Heinrich-Buff-Ring 16, D-35392 Giessen, Germany*
³¹ *Lanzhou University, Lanzhou 730000, People's Republic of China*
³² *Liaoning Normal University, Dalian 116029, People's Republic of China*
³³ *Liaoning University, Shenyang 110036, People's Republic of China*
³⁴ *Nanjing Normal University, Nanjing 210023, People's Republic of China*
³⁵ *Nanjing University, Nanjing 210093, People's Republic of China*
³⁶ *Nankai University, Tianjin 300071, People's Republic of China*
³⁷ *National Centre for Nuclear Research, Warsaw 02-093, Poland*
³⁸ *North China Electric Power University, Beijing 102206, People's Republic of China*
³⁹ *Peking University, Beijing 100871, People's Republic of China*
⁴⁰ *Qufu Normal University, Qufu 273165, People's Republic of China*
⁴¹ *Shandong Normal University, Jinan 250014, People's Republic of China*
⁴² *Shandong University, Jinan 250100, People's Republic of China*
⁴³ *Shanghai Jiao Tong University, Shanghai 200240, People's Republic of China*
⁴⁴ *Shanxi Normal University, Linfen 041004, People's Republic of China*
⁴⁵ *Shanxi University, Taiyuan 030006, People's Republic of China*
⁴⁶ *Sichuan University, Chengdu 610064, People's Republic of China*
⁴⁷ *Soochow University, Suzhou 215006, People's Republic of China*
⁴⁸ *South China Normal University, Guangzhou 510006, People's Republic of China*
⁴⁹ *Southeast University, Nanjing 211100, People's Republic of China*
⁵⁰ *State Key Laboratory of Particle Detection and Electronics, Beijing 100049, Hefei 230026, People's Republic of China*
⁵¹ *Sun Yat-Sen University, Guangzhou 510275, People's Republic of China*
⁵² *Suranaree University of Technology, University Avenue 111, Nakhon Ratchasima 30000, Thailand*
⁵³ *Tsinghua University, Beijing 100084, People's Republic of China*
⁵⁴ *Turkish Accelerator Center Particle Factory Group, (A)Istinye University, 34010, Istanbul, Turkey; (B)Near East University, Nicosia, North Cyprus, Mersin 10, Turkey*

- ⁵⁵ *University of Chinese Academy of Sciences, Beijing 100049, People's Republic of China*
- ⁵⁶ *University of Groningen, NL-9747 AA Groningen, The Netherlands*
- ⁵⁷ *University of Hawaii, Honolulu, Hawaii 96822, USA*
- ⁵⁸ *University of Jinan, Jinan 250022, People's Republic of China*
- ⁵⁹ *University of Manchester, Oxford Road, Manchester, M13 9PL, United Kingdom*
- ⁶⁰ *University of Minnesota, Minneapolis, Minnesota 55455, USA*
- ⁶¹ *University of Muenster, Wilhelm-Klemm-Str. 9, 48149 Muenster, Germany*
- ⁶² *University of Oxford, Keble Rd, Oxford, UK OX13RH*
- ⁶³ *University of Science and Technology Liaoning, Anshan 114051, People's Republic of China*
- ⁶⁴ *University of Science and Technology of China, Hefei 230026, People's Republic of China*
- ⁶⁵ *University of South China, Hengyang 421001, People's Republic of China*
- ⁶⁶ *University of the Punjab, Lahore-54590, Pakistan*
- ⁶⁷ *University of Turin and INFN, (A)University of Turin, I-10125, Turin, Italy; (B)University of Eastern Piedmont, I-15121, Alessandria, Italy; (C)INFN, I-10125, Turin, Italy*
- ⁶⁸ *Uppsala University, Box 516, SE-75120 Uppsala, Sweden*
- ⁶⁹ *Wuhan University, Wuhan 430072, People's Republic of China*
- ⁷⁰ *Xinyang Normal University, Xinyang 464000, People's Republic of China*
- ⁷¹ *Yunnan University, Kunming 650500, People's Republic of China*
- ⁷² *Zhejiang University, Hangzhou 310027, People's Republic of China*
- ⁷³ *Zhengzhou University, Zhengzhou 450001, People's Republic of China*
- ^a *Also at the Moscow Institute of Physics and Technology, Moscow 141700, Russia*
- ^b *Also at the Novosibirsk State University, Novosibirsk, 630090, Russia*
- ^c *Also at the NRC "Kurchatov Institute", PNPI, 188300, Gatchina, Russia*
- ^d *Currently at Istanbul Arel University, 34295 Istanbul, Turkey*
- ^e *Also at Goethe University Frankfurt, 60323 Frankfurt am Main, Germany*
- ^f *Also at Key Laboratory for Particle Physics, Astrophysics and Cosmology, Ministry of Education; Shanghai Key Laboratory for Particle Physics and Cosmology; Institute of Nuclear and Particle Physics, Shanghai 200240, People's Republic of China*
- ^g *Also at Key Laboratory of Nuclear Physics and Ion-beam Application (MOE) and Institute of Modern Physics, Fudan University, Shanghai 200443, People's Republic of China*
- ^h *Also at State Key Laboratory of Nuclear Physics and Technology, Peking University, Beijing 100871, People's Republic of China*
- ⁱ *Also at School of Physics and Electronics, Hunan University, Changsha 410082, China*
- ^j *Also at Guangdong Provincial Key Laboratory of Nuclear Science, Institute of Quantum Matter, South China Normal University, Guangzhou 510006, China*
- ^k *Also at Frontiers Science Center for Rare Isotopes, Lanzhou University, Lanzhou 730000, People's Republic of China*
- ^l *Also at Lanzhou Center for Theoretical Physics, Lanzhou University, Lanzhou 730000, People's Republic of China*
- ^m *Also at the Department of Mathematical Sciences, IBA, Karachi, Pakistan*

Based on $(10087 \pm 44) \times 10^6$ J/ψ events collected with the BESIII detector, the process $J/\psi \rightarrow \gamma\pi^+\pi^-\eta'$ is studied using two dominant decay channels of the η' meson, $\eta' \rightarrow \gamma\pi^+\pi^-$ and $\eta' \rightarrow \eta\pi^+\pi^-$, $\eta \rightarrow \gamma\gamma$. The $X(2600)$ is observed with a statistical significance larger than 20σ in the $\pi^+\pi^-\eta'$ invariant mass spectrum, and it has a strong correlation to a structure around $1.5 \text{ GeV}/c^2$ in the $\pi^+\pi^-$ invariant mass spectrum. A simultaneous fit on the $\pi^+\pi^-\eta'$ and $\pi^+\pi^-$ invariant mass spectra with the two η' decay modes indicates that the mass and width of the $X(2600)$ state are $2617.8 \pm 2.1_{-1.9}^{+18.2} \text{ MeV}/c^2$ and $200 \pm 8_{-17}^{+20} \text{ MeV}$, respectively. The corresponding branching fractions are measured to be $B(J/\psi \rightarrow \gamma X(2600)) \cdot B(X(2600) \rightarrow f_0(1500)\eta') \cdot B(f_0(1500) \rightarrow \pi^+\pi^-) = (3.39 \pm 0.18_{-0.66}^{+0.91}) \times 10^{-5}$ and $B(J/\psi \rightarrow \gamma X(2600)) \cdot B(X(2600) \rightarrow f_2'(1525)\eta') \cdot B(f_2'(1525) \rightarrow \pi^+\pi^-) = (2.43 \pm 0.13_{-1.11}^{+0.31}) \times 10^{-5}$, where the first uncertainties are statistical, and the second systematic.

Radiative decays of the J/ψ meson are ideally suited for light hadron spectroscopy studies, including in particular searches for exotic hadrons, e.g. of glueballs and hybrids [1, 2]. The $\pi^+\pi^-\eta'$ mode is of special interest since it is one of the most favorite modes to search for a pseudoscalar glueball [3, 4]. Lattice Quantum Chromodynamics(LQCD) predicts that the ground state of the 0^{-+} glueballs has a mass around $2.3 - 2.6 \text{ GeV}/c^2$ [5–8]. Therefore, it is important to search for all possible mesons in the $2.3 - 2.6 \text{ GeV}/c^2$ region in $J/\psi \rightarrow \gamma\pi^+\pi^-\eta'$

decays with the unprecedented sample of J/ψ events collected at BESIII.

In the process $J/\psi \rightarrow \gamma\pi^+\pi^-\eta'$, a set of exotic states have been observed. The $X(1835)$ resonance was first observed by the BES collaboration [9] with a statistical significance of 7.7σ and confirmed with a statistical significance larger than 20σ by the BESIII collaboration [10]. The $X(2120)$ and $X(2370)$ resonances were first observed with statistical significances of 7.2σ and 6.4σ , respectively, by the BESIII collaboration [10]. The spin

parity of the $X(1835)$ resonance is determined to be 0^{-+} in the process $J/\psi \rightarrow \gamma K_S^0 K_S^0 \eta$ [11]. The theoretical interpretation of $X(1835)$ is still in question. Possibilities include a $p\bar{p}$ bound state [12], a second radial excitation of the η' [13] and a pseudoscalar glueball [14]. The measured mass of $X(2370)$ is consistent with the LQCD prediction for the pseudoscalar glueball [7]. Further observations of the process $J/\psi \rightarrow \gamma\pi^+\pi^-\eta'$ are important to help the understanding of QCD and hadronic physics.

In this Letter, the process $J/\psi \rightarrow \gamma\pi^+\pi^-\eta'$ is studied with two dominant η' decay modes, $\eta' \rightarrow \gamma\pi^+\pi^-$ and $\eta' \rightarrow \pi^+\pi^-\eta$, $\eta \rightarrow \gamma\gamma$ using the J/ψ data sample collected with the BESIII detector in the years of 2009, 2012, 2018 and 2019. The number of J/ψ decays is $(10087 \pm 44) \times 10^6$ [15]. A resonance, the $X(2600)$, is observed in the $\pi^+\pi^-\eta'$ invariant mass spectrum.

The BESIII detector [16] records symmetric e^+e^- collisions provided by the BEPCII storage ring [17], which operates with a peak luminosity of $1 \times 10^{33} \text{ cm}^{-2}\text{s}^{-1}$ in the center-of-mass energy range from 2.0 to 4.7 GeV. The cylindrical core of the BESIII detector covers 93% of the full solid angle and consists of a helium-based multilayer drift chamber (MDC), a plastic scintillator time-of-flight system (TOF), and a CsI(Tl) electromagnetic calorimeter (EMC), which are all enclosed in a superconducting solenoidal magnet providing a 1.0 T (0.9 T in 2012) magnetic field. The solenoid is supported by an octagonal flux-return yoke with resistive plate counter muon identification modules interleaved with steel. The charged-particle momentum resolution at 1 GeV/c is 0.5%, and the dE/dx resolution is 6% for electrons from Bhabha scattering. The EMC measures photon energies with a resolution of 2.5% (5%) at 1 GeV in the barrel (end cap) region. The time resolution in the TOF barrel region is 68 ps, while that in the end cap region is 110 ps. The end cap TOF system was upgraded in 2015 using multi-gap resistive plate chamber technology, providing a time resolution of 60 ps [18–20].

Simulated data samples produced with GEANT4-based [21] Monte Carlo (MC) software, which includes the geometric description of the BESIII detector and the detector response, are used to determine detection efficiencies and to estimate backgrounds. The simulation models the beam energy spread and initial state radiation in the e^+e^- annihilations with the generator KKMC [22, 23]. An inclusive MC sample includes both the production of the J/ψ resonance and the continuum processes incorporated in KKMC [22, 23]. The known decay modes are modeled with EVTGEN [24, 25] using branching fractions taken from the Particle Data Group (PDG) [26], and the remaining unknown charmonium decays are modeled with LUNDCHARM [27, 28]. Final state radiation from charged final state particles is incorporated using PHOTOS [29].

Charged tracks detected in the MDC are required to be within the polar angle (θ) range of $|\cos\theta| < 0.93$, where θ is defined with respect to the z -axis, which is

the symmetry axis of the MDC. The distance of closest approach to the interaction point must be less than 10 cm along the z -axis and less than 1 cm in the transverse plane. Particle identification (PID) for charged tracks combines measurements of the dE/dx in the MDC and the flight time in the TOF to form likelihoods for each hadron (p , K and π) hypothesis; each track is assigned to the particle type that corresponds to the hypothesis with the highest confidence level. Photon candidates are identified using showers in the EMC. The deposited energy of each shower must be more than 25 MeV in the barrel region ($|\cos\theta| < 0.8$) and more than 50 MeV in the end cap region ($0.86 < |\cos\theta| < 0.92$). To suppress electronic noise and showers unrelated to the event, the difference between the EMC time and the event start time is required to be within (0, 700) ns.

For the $J/\psi \rightarrow \gamma\pi^+\pi^-\eta'$, $\eta' \rightarrow \gamma\pi^+\pi^-$ channel, event candidates are required to have four charged tracks with at least three charged tracks identified as pions and at least two photons with energies larger than 100 MeV. A four-constraint (4C) kinematic fit, which constrains the total four-momentum of all final state particles to the initial four-momentum of the e^+e^- system, is performed to the $\gamma\gamma\pi^+\pi^-\pi^+\pi^-$ hypothesis. If there are more than two photons, the combination that has the smallest χ_{4C}^2 will be chosen, and $\chi_{4C}^2 < 40$ is required. The η' candidates require $|M_{\gamma\pi^+\pi^-} - m_{\eta'}| < 15 \text{ MeV}/c^2$, where $m_{\eta'}$ is the mass of η' reported by the PDG [26]. If there is more than one $\gamma\pi^+\pi^-$ combination passing the above criteria, the combination with minimum $|M_{\gamma\pi^+\pi^-} - m_{\eta'}|$ will be selected. For the photons of the selected combination, the requirements $|M_{\gamma\gamma} - m_{\pi^0}| > 40 \text{ MeV}/c^2$, $|M_{\gamma\gamma} - m_{\eta}| > 30 \text{ MeV}/c^2$, and $720 < M_{\gamma\gamma} < 820 \text{ MeV}/c^2$, where m_{π^0} and m_{η} are the masses of π^0 and η mesons from the PDG [26], are used to suppress the backgrounds from the processes of $J/\psi \rightarrow \pi^0\pi^+\pi^-\pi^+\pi^-$, $J/\psi \rightarrow \eta\pi^+\pi^-\pi^+\pi^-$, and $J/\psi \rightarrow \omega(\omega \rightarrow \gamma\pi^0)\pi^+\pi^-\pi^+\pi^-$. The requirement of $400 \text{ MeV}/c^2 < M_{\gamma\pi^+\pi^-} < 563 \text{ MeV}/c^2$ is used to suppress the background from the processes of $J/\psi \rightarrow \gamma\eta(\eta \rightarrow \gamma\pi^+\pi^-\pi^+\pi^-)$ and $J/\psi \rightarrow \gamma\eta(\eta \rightarrow \pi^0\pi^+\pi^-)\pi^+\pi^-$. In order to suppress the background from $J/\psi \rightarrow \pi^0\pi^+\pi^-\eta'$ decays, the J/ψ radiative photon is paired with all additional photons, and events with any pairing with $|M_{\gamma\gamma} - m_{\pi^0}| < 15 \text{ MeV}/c^2$ are rejected. After application of the above selection criteria, there are evident signatures of the $X(1835)$, $X(2120)$, $X(2370)$, as well as a distinct signal of the η_c meson in the $\pi^+\pi^-\eta'$ invariant mass spectrum, shown in Fig. 1(a), which are consistent with previous BESIII results [10]. In addition, there is a structure around 2.6 GeV/ c^2 , the $X(2600)$, in the $\pi^+\pi^-\eta'$ invariant mass spectrum, which is strongly correlated to a structure around 1.5 GeV/ c^2 in the $\pi^+\pi^-$ invariant mass spectrum as shown in Fig. 1(c).

For the $J/\psi \rightarrow \gamma\pi^+\pi^-\eta'$, $\eta' \rightarrow \pi^+\pi^-\eta$, $\eta \rightarrow \gamma\gamma$ channel, event candidates are required to have four charged tracks with at least three charged tracks identified as

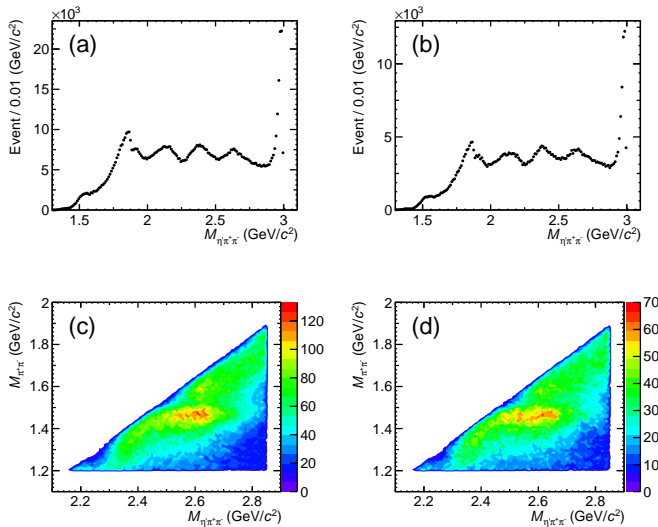


FIG. 1. The $J/\psi \rightarrow \gamma\pi^+\pi^-\eta'$ candidates in data: (top) the invariant mass spectrum of the final state $\pi^+\pi^-\eta'$ after event selection (a) with the $\eta' \rightarrow \gamma\pi^+\pi^-$ channel, (b) with the $\eta' \rightarrow \pi^+\pi^-\eta$ channel, and (bottom) the two dimensional distribution of $M_{\pi^+\pi^-}$ versus $M_{\pi^+\pi^-\eta'}$ with $M_{\pi^+\pi^-} > 1.2 \text{ GeV}/c^2$ and $2.2 < M_{\pi^+\pi^-\eta'} < 2.85 \text{ GeV}/c^2$ (c) with the $\eta' \rightarrow \gamma\pi^+\pi^-$ channel and (d) with the $\eta' \rightarrow \pi^+\pi^-\eta$ channel.

pions and at least three photons with energies larger than 100 MeV. A 4C kinematic fit is performed to the $\gamma\gamma\pi^+\pi^-\pi^+\pi^-$ hypothesis. If there are more than three photon candidates, the combination with the smallest χ_{4C}^2 will be chosen, and $\chi_{4C}^2 < 40$ is required. The η candidates are reconstructed with the requirement of $|M_{\gamma\gamma} - m_\eta| < 30 \text{ MeV}/c^2$. For the three selected photons, the requirement $|M_{\gamma\gamma} - m_{\pi^0}| > 40 \text{ MeV}/c^2$ is used for all photon pairs to suppress the π^0 background. Besides the 4C kinematic fit, a five-constraint (5C) kinematic fit is performed, in which in addition to the constraint on the total four momentum of the final-state particles, the invariant mass of two photons coming from η is constrained to m_η . If more than one combination is found in an event, the combination with the minimum χ_{5C}^2 will be selected, and $\chi_{5C}^2 < 40$ is required. To select η' candidates, $|M_{\pi^+\pi^-\eta} - m_{\eta'}| < 10 \text{ MeV}/c^2$ is required. If there is more than one $\pi^+\pi^-\eta$ combination passing the above criteria, the combination with smallest $|M_{\pi^+\pi^-\eta} - m_{\eta'}|$ will be selected as the η' candidate. In order to suppress the background from the processes of $J/\psi \rightarrow \pi^0\pi^+\pi^-\eta'$, the J/ψ radiative photon is paired with all additional photons, and events with any pair with $|M_{\gamma\gamma} - m_{\pi^0}| < 15 \text{ MeV}/c^2$ are rejected. After the above selection criteria, the $\pi^+\pi^-\eta'$ mass spectrum as shown in Fig. 1(b) is similar to that in the $\eta' \rightarrow \gamma\pi^+\pi^-$ channel. There is a structure around $2.6 \text{ GeV}/c^2$, the $X(2600)$, in the $\pi^+\pi^-\eta'$ invariant mass spectrum, which is strongly correlated with the structure

around $1.5 \text{ GeV}/c^2$ in the $\pi^+\pi^-$ invariant mass spectrum as shown in Fig. 1(d).

Possible background contributions are studied using an inclusive MC sample. There are two kinds of background. One is from non- η' processes and the other is from the process $J/\psi \rightarrow \pi^0\pi^+\pi^-\eta'$. The former one can be estimated with the η' side-band regions in data, which are chosen to be $30 < |M_{\gamma\pi^+\pi^-} - m_{\eta'}| < 45 \text{ MeV}/c^2$ for the channel of $\eta' \rightarrow \gamma\pi^+\pi^-$, and $20 < |M_{\pi^+\pi^-\eta} - m_{\eta'}| < 30 \text{ MeV}/c^2$ for the $\eta' \rightarrow \pi^+\pi^-\eta$, $\eta \rightarrow \gamma\gamma$ channel. Background coming from $J/\psi \rightarrow \pi^0\pi^+\pi^-\eta'$ decays can pass the final selection criteria for $J/\psi \rightarrow \gamma\pi^+\pi^-\eta'$ decays if one of the photons from the π^0 decay is not reconstructed or is out of the detector acceptance. To estimate the background contribution from the $J/\psi \rightarrow \pi^0\pi^+\pi^-\eta'$ decays, we use a control sample of decays passing the selection criteria for $J/\psi \rightarrow \gamma\pi^+\pi^-\eta'$ decays, but with a reversed π^0 veto criterium, $|M_{\gamma\gamma} - m_{\pi^0}| < 15 \text{ MeV}/c^2$. The residual $\pi^0\pi^+\pi^-\eta'$ background contribution in the $J/\psi \rightarrow \gamma\pi^+\pi^-\eta'$ signal region can be estimated by reweighting the events from the control sample. The weight factors are dependent on the radiative photon energy, and equal to the MC efficiency ratio of the $J/\psi \rightarrow \gamma\pi^+\pi^-\eta'$ signal selection and the $J/\psi \rightarrow \pi^0\pi^+\pi^-\eta'$ background sample selection. Neither of these background components produces a peaking structure in the $\pi^+\pi^-\eta'$ and $\pi^+\pi^-$ invariant mass spectrum.

In order to determine the signal of the $X(2600)$ resonance with a consequent decay to a resonance at mass around $1.5 \text{ GeV}/c^2$ in the $\pi^+\pi^-$ invariant mass spectrum, a simultaneous fit to the $\pi^+\pi^-\eta'$ and $\pi^+\pi^-$ mass spectra is performed, including the two decay channels of $\eta' \rightarrow \gamma\pi^+\pi^-$ and $\eta' \rightarrow \pi^+\pi^-\eta$, $\eta \rightarrow \gamma\gamma$. In the fit, the number of events is the same in the two projected mass spectra for a given channel. Moreover, the mass, width and branching fraction of each resonance are common between the two η' decay channels in the simultaneous fit. The line shape of the $X(2600)$ resonance in the $\pi^+\pi^-\eta'$ mass spectrum is described with an efficiency-corrected Breit-Wigner function convolved with a double Gaussian function describing the detector resolution. The FWHM (full width at half maximum) resolution on the $M_{\pi^+\pi^-\eta'}$ distribution is around $10 \text{ MeV}/c^2$. The structure around $1.5 \text{ GeV}/c^2$ in the $\pi^+\pi^-$ mass spectrum is described with an efficiency-corrected interference between the $f_0(1500)$ and the $f_2'(1525)$ convolved with a double Gaussian function describing the detector resolution. The $M_{\pi^+\pi^-}$ FWHM resolution is about $9 \text{ MeV}/c^2$. Two Breit-Wigner functions are used to describe the line shape of $f_0(1500)$ and $f_2'(1525)$. The mass and width of the $f_2'(1525)$ are fixed to the PDG values [26], while the mass and width of the $f_0(1500)$ are floated in the fit, given the large discrepancy between different experiments [30–34]. The contributions from other processes with the $\gamma\pi^+\pi^-\eta'$ final state are described with two different fourth order polynomial functions in the $\pi^+\pi^-\eta'$

and $\pi^+\pi^-$ mass spectra, and are treated as incoherent. The background contributions from the non- η' events and $J/\psi \rightarrow \pi^0\pi^+\pi^-\eta'$ decays are estimated with the two different methods as described earlier, and both the mass line shapes and yields are fixed in the fit.

Figure 2 shows the simultaneous fit results with the two η' decay modes in the region with $M_{\pi^+\pi^-} > 1.2$ GeV/ c^2 and $2.3 < M_{\pi^+\pi^-\eta'} < 2.85$ GeV/ c^2 . The statistical significance is determined from the change of $-2\ln L$ (L is the combined likelihood of simultaneous fit) in the fit with and without signal assumption, considering the change of degrees of freedom of the fits. The significances of the $X(2600)$, $f_0(1500)$ and $f_2'(1525)$ resonances are all larger than 20σ . The mass and width of the $X(2600)$ are $2617.8 \pm 2.1(\text{stat.})$ MeV/ c^2 and $200 \pm 8(\text{stat.})$ MeV, respectively, and those of the $f_0(1500)$ are $1498.0 \pm 4.5(\text{stat.})$ MeV/ c^2 and $166 \pm 10(\text{stat.})$ MeV, respectively. The masses and widths are summarized in Table I. The branching fractions are measured to be $B(J/\psi \rightarrow \gamma X(2600)) \cdot B(X(2600) \rightarrow f_0(1500)\eta') \cdot B(f_0(1500) \rightarrow \pi^+\pi^-) = (3.39 \pm 0.18(\text{stat.})) \times 10^{-5}$ and $B(J/\psi \rightarrow \gamma X(2600)) \cdot B(X(2600) \rightarrow f_2'(1525)\eta') \cdot B(f_2'(1525) \rightarrow \pi^+\pi^-) = (2.43 \pm 0.13(\text{stat.})) \times 10^{-5}$. The numbers of signal events, efficiencies, and branching fractions are listed in Table II.

The consistency between the two η' decay channels is verified by fitting the two channels separately with the method described above. The fit to the $\eta' \rightarrow \gamma\pi^+\pi^-$ channel gives $M = 2619.5 \pm 2.3(\text{stat.})$ MeV/ c^2 and $\Gamma = 185 \pm 10(\text{stat.})$ MeV. For the fit to the $\eta' \rightarrow \pi^+\pi^-\eta$ channel, the mass and width of $X(2600)$ are determined to be $M = 2616.1 \pm 3.9(\text{stat.})$ MeV/ c^2 and $\Gamma = 206 \pm 13(\text{stat.})$ MeV. The statistical significances of the two η' decay channels are both greater than 10σ . The masses and widths of the $X(2600)$ are in good agreement between the two η' decay channels.

The systematic uncertainties of the mass and width are mainly from the fit strategy, fit range, background estimation, phase space of $J/\psi \rightarrow \gamma\pi^+\pi^-\eta'$ decays, line shape of the intermediate resonance $f_2'(1525)$, quantum number assumption of the $X(2600)$ state and treatment of the contribution from the other processes with the final state of $\gamma\pi^+\pi^-\eta'$. The uncertainties are determined by including an additional resonance in the fit, using different parameters for the $f_2'(1525)$ line shape, a different quantum number assignment for the $X(2600)$, and different treatment of the contribution from the other processes, as well as varying the fit range, side-band region, etc.. The dominant uncertainty sources are from including an additional resonance in the fit and assuming different quantum numbers for the $X(2600)$. To estimate the uncertainty from the fit with the additional resonance, the $X(2370)$ is included into the simultaneous fit, and interference between the $X(2370)$ and the $X(2600)$ is included. Two different hypotheses for the quantum numbers of $X(2600)$, 0^{-+} and 2^{-+} , are used

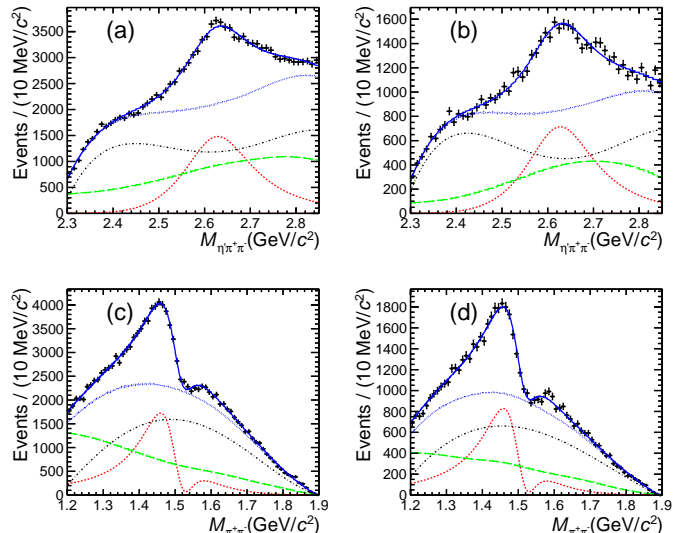


FIG. 2. The $\pi^+\pi^-\eta'$ and $\pi^+\pi^-$ mass spectra distributions with the two decay channels of η' , $\eta' \rightarrow \gamma\pi^+\pi^-$ and $\eta' \rightarrow \pi^+\pi^-\eta$, with the simultaneous fit results overlaid: (a) and (c) are fit results for $\eta' \rightarrow \gamma\pi^+\pi^-$ channel, (b) and (d) are fit results for the $\eta' \rightarrow \pi^+\pi^-\eta$ channel. The dots with error bar are data, the blue solid lines are the total fits, the red dashed lines describe the $X(2600)$ signal in the $\pi^+\pi^-\eta'$ mass spectrum, and the structure around 1.5 GeV/ c^2 in $\pi^+\pi^-$ mass spectrum, the black dash-dotted lines correspond to the background described by a polynomial function, and the green long dashed lines are $J/\psi \rightarrow \pi^0\pi^+\pi^-\eta'$ and non- η' background, the blue dotted lines are the total background, including the $J/\psi \rightarrow \pi^0\pi^+\pi^-\eta'$, non- η' background and polynomial background.

in the simultaneous fit, the difference between them is treated as the uncertainty caused by the quantum number assumption for the $X(2600)$ state. The largest deviations from the baseline case are taken as the systematic errors. The total uncertainties on the mass and width of the $X(2600)$ are $^{+18.2}_{-1.9}$ MeV/ c^2 and $^{+20}_{-17}$ MeV.

To estimate the systematic error of the branching fraction measurement, additional uncertainties are considered, including the data-MC difference in the charged track reconstruction efficiency, photon detection efficiency, PID efficiency, the kinematic fit and the number of J/ψ events. The total systematic uncertainties on the branching fraction are $^{+27\%}_{-20\%}$ and $^{+13\%}_{-47\%}$ for the $B(J/\psi \rightarrow \gamma X(2600)) \cdot B(X(2600) \rightarrow f_0(1500)\eta') \cdot B(f_0(1500) \rightarrow \pi^+\pi^-)$ and $B(J/\psi \rightarrow \gamma X(2600)) \cdot B(X(2600) \rightarrow f_2'(1525)\eta') \cdot B(f_2'(1525) \rightarrow \pi^+\pi^-)$, respectively.

In summary, the process $J/\psi \rightarrow \gamma\pi^+\pi^-\eta'$, with $\eta' \rightarrow \gamma\pi^+\pi^-$ and $\eta' \rightarrow \pi^+\pi^-\eta$, $\eta \rightarrow \gamma\gamma$, is studied with $(10087 \pm 44) \times 10^6$ J/ψ events collected by the BESIII detector. A resonance, the $X(2600)$, is observed for the first time, with a statistical significance greater than 20σ . There is a strong correlation between the $X(2600)$

Case	$f_0(1500)$	$X(2600)$
Mass (MeV/ c^2)	$1498.0 \pm 4.5_{-15.2}^{+4.0}$	$2617.8 \pm 2.1_{-1.9}^{+18.2}$
Width (MeV)	$166 \pm 10_{-26}^{+13}$	$200 \pm 8_{-17}^{+20}$

TABLE I. Masses and widths of the $f_0(1500)$ and $X(2600)$. The first uncertainties are statistical, and the second are systematic.

Case	$f_0(1500)$	$f_2'(1525)$
Events	26917 ± 1069	19094 ± 759
Efficiency	19%	15%
BF ($\times 10^{-5}$)	$3.39 \pm 0.18_{-0.66}^{+0.91}$	$2.43 \pm 0.13_{-1.11}^{+0.31}$

TABLE II. Branching fractions for $J/\psi \rightarrow \gamma X(2600)$, $X(2600) \rightarrow f_0(1500)/f_2'(1525)\eta'$, $f_0(1500)/f_2'(1525) \rightarrow \pi^+\pi^-$. BF is the product of the three branching fractions involved. The first uncertainties are statistical, and the second are systematic.

and the structure at 1.5 GeV/ c^2 in the $\pi^+\pi^-$ invariant mass spectrum. A simultaneous fit of the $\pi^+\pi^-\eta'$ and $\pi^+\pi^-$ mass spectra with the two η' decay channels of $\eta' \rightarrow \gamma\pi^+\pi^-$ and $\eta' \rightarrow \pi^+\pi^-\eta$ is performed. The structure around 1.5 GeV/ c^2 in the $\pi^+\pi^-$ invariant mass spectra can be well described with the interference between the $f_0(1500)$ and the $f_2'(1525)$ resonances. The masses and width of the $X(2600)$ and $f_0(1500)$ resonances are listed in Table I, and the product branching fractions $B(J/\psi \rightarrow \gamma X(2600)) \cdot B(X(2600) \rightarrow f_0(1500)/f_2'(1525)\eta') \cdot B(f_0(1500)/f_2'(1525) \rightarrow \pi^+\pi^-)$ are listed in Table II.

With these decay modes, the spin parity assignment of 0^{-+} or 2^{-+} is favored for the $X(2600)$. In order to understand the nature of the $X(2600)$ state, whether it can be interpreted as an η radial excitation [35], or a potential exotic hadron, it is important to determine its spin-parity and to study its production and decay properties in other J/ψ decay channels.

The BESIII collaboration thanks the staff of BEPCII and the IHEP computing center for their strong support. This work is supported in part by National Key Research and Development Program of China under Contracts Nos. 2020YFA0406300, 2020YFA0406400; National Natural Science Foundation of China (NSFC) under Contracts Nos. 11625523, 11635010, 11735014, 11822506, 11835012, 11935015, 11935016, 11935018, 11961141012, 12022510, 12025502, 12035009, 12035013, 12061131003; the Chinese Academy of Sciences (CAS) Large-Scale Scientific Facility Program; Joint Large-Scale Scientific Facility Funds of the NSFC and CAS under Contracts Nos. U1732263, U1832207; CAS Key Research Program of Frontier Sciences under Contract No. QYZDJ-SSW-SLH040; 100 Talents Program of CAS; INPAC and Shanghai Key Laboratory for Particle Physics and Cos-

mology; ERC under Contract No. 758462; European Union Horizon 2020 research and innovation programme under Contract No. Marie Skłodowska-Curie grant agreement No 894790; German Research Foundation DFG under Contracts Nos. 443159800, Collaborative Research Center CRC 1044, GRK 214; Istituto Nazionale di Fisica Nucleare, Italy; Ministry of Development of Turkey under Contract No. DPT2006K-120470; National Science and Technology fund; Olle Engkvist Foundation under Contract No. 200-0605; STFC (United Kingdom); The Knut and Alice Wallenberg Foundation (Sweden) under Contract No. 2016.0157; The Royal Society, UK under Contracts Nos. DH140054, DH160214; The Swedish Research Council; U. S. Department of Energy under Contracts Nos. DE-FG02-05ER41374, DE-SC-0012069.

-
- [1] M. B. Çakır and G. R. Farrar, *Phys. Rev. D* **50**, 3268 (1994).
 - [2] F. E. Close, G. R. Farrar, and Z. Li, *Phys. Rev. D* **55**, 5749 (1997).
 - [3] C. Amsler and N. A. Törnqvist, *Physics Reports* **389**, 61 (2004).
 - [4] W. I. Eshraim, S. Janowski, F. Giacosa, and D. H. Rischke, *Phys. Rev. D* **87**, 054036 (2013), [arXiv:1208.6474 \[hep-ph\]](https://arxiv.org/abs/1208.6474).
 - [5] G. S. Bali, K. Schilling, A. Hulsebos, A. C. Irving, C. Michael, and P. W. Stephenson (UKQCD Collaboration), *Phys. Lett. B* **309**, 378 (1993).
 - [6] C. J. Morningstar and M. J. Peardon, *Phys. Rev. D* **60**, 034509 (1999).
 - [7] Y. Chen *et al.*, *Phys. Rev. D* **73**, 014516 (2006).
 - [8] E. Gregory, A. Irving, B. Lucini, C. McNeile, A. Rago, C. Richards, and E. Rinaldi, *JHEP* **10**, 170 (2012).
 - [9] M. Ablikim *et al.* (BES Collaboration), *Phys. Rev. Lett.* **95**, 262001 (2005).
 - [10] M. Ablikim *et al.* (BESIII Collaboration), *Phys. Rev. Lett.* **106**, 072002 (2011).
 - [11] M. Ablikim *et al.* (BESIII Collaboration), *Phys. Rev. Lett.* **115**, 091803 (2015).
 - [12] S. L. Zhu and C. S. Gao, *Commun. Theor. Phys.* **46**, 291 (2006).
 - [13] T. Huang and S. L. Zhu, *Phys. Rev. D* **73**, 014023 (2006).
 - [14] N. Kochelev and D. P. Min, *Physics Letters B* **633**, 283 (2006).
 - [15] M. Ablikim *et al.* (BESIII Collaboration), *Chin. Phys. C* **41**, 013001 (2017).
 - [16] M. Ablikim *et al.* (BESIII Collaboration), *Nuclear Instruments and Methods in Physics Research Section A: Accelerators, Spectrometers, Detectors and Associated Equipment* **614**, 345 (2010).
 - [17] C. H. Yu *et al.*, in *Proceedings of IPAC2016, Busan, Korea, 2016*.
 - [18] X. Li *et al.*, *Radiat. Detect. Technol. Methods* **1**, 13 (2017).
 - [19] Y. X. Guo *et al.*, *Radiat. Detect. Technol. Methods* **1**, 15 (2017).
 - [20] P. Cao *et al.*, *Nuclear Instruments and Methods in Physics Research Section A: Accelerators, Spectrometers, Detectors and Associated Equipment* **614**, 345 (2010).

- ters, *Nuclear Instruments and Associated Equipment* **953**, 163053 (2020).
- [21] S. Agostinelli *et al.*, *Nuclear Instruments and Methods in Physics Research Section A: Accelerators, Spectrometers, Detectors and Associated Equipment* **506**, 250 (2003).
- [22] S. Jadach, B. F. L. Ward, and Z. Was, *Phys. Rev. D* **63**, 113009 (2001).
- [23] S. Jadach, B. F. L. Ward, and Z. Was, *Computer Physics Communications* **130**, 260 (2000).
- [24] D. J. Lange, *Nuclear Instruments and Methods in Physics Research Section A: Accelerators, Spectrometers, Detectors and Associated Equipment* **462**, 152 (2001).
- [25] R. G. Ping, *Chinese Physics C* **32**, 599 (2008).
- [26] Particle Data Group, *Progress of Theoretical and Experimental Physics* **2020** (2020), 10.1093/ptep/ptaa104, 083C01.
- [27] J. C. Chen, G. S. Huang, X. R. Qi, D. H. Zhang, and Y. S. Zhu, *Phys. Rev. D* **62**, 034003 (2000).
- [28] R. L. Yang, R. G. Ping, and H. Chen, *Chinese Physics Letters* **31**, 061301 (2014).
- [29] E. Barberio and Z. Was, *Comput. Phys. Commun.* **79**, 291 (1994).
- [30] M. Ablikim *et al.* (BES Collaboration), *Phys. Lett. B* **642**, 441 (2006).
- [31] M. Ablikim *et al.* (BESIII Collaboration), *Phys. Rev. D* **87**, 092009 (2013).
- [32] R. Aaij *et al.* (LHCb Collaboration), *Phys. Rev. D* **89**, 092006 (2014).
- [33] A. Bertin *et al.* (OBELIX Collaboration), *Phys. Rev. D* **57**, 55 (1998).
- [34] B. Aubert *et al.* (BaBar Collaboration), *Phys. Rev. D* **74**, 032003 (2006).
- [35] L. M. Wang, Q. S. Zhou, C. Q. Pang, and X. Liu, *Phys. Rev. D* **102**, 114034 (2020).